

Article

**Regioselectivity in Azahydro[60]fullerene Derivatives:
Application of General-Purpose Reactivity Indicators**

Flavio F. Contreras-Torres, Vladimir A. Basiuk, and Elena V. Basiuk

J. Phys. Chem. A, **2008**, 112 (35), 8154-8163 • DOI: 10.1021/jp8047967 • Publication Date (Web): 08 August 2008

Downloaded from <http://pubs.acs.org> on December 8, 2008

More About This Article

Additional resources and features associated with this article are available within the HTML version:

- Supporting Information
- Access to high resolution figures
- Links to articles and content related to this article
- Copyright permission to reproduce figures and/or text from this article

[View the Full Text HTML](#)



ACS Publications
High quality. High impact.

The Journal of Physical Chemistry A is published by the American Chemical Society, 1155 Sixteenth Street N.W., Washington, DC 20036

Regioselectivity in Azahydro[60]fullerene Derivatives: Application of General-Purpose Reactivity Indicators

Flavio F. Contreras-Torres,^{*,†,‡} Vladimir A. Basiuk,[‡] and Elena V. Basiuk[†]

Centro de Ciencias Aplicadas y Desarrollo Tecnológico and Instituto de Ciencias Nucleares, Universidad Nacional Autónoma de México, Circuito Exterior C. U., 04510 México D.F., Mexico

Received: May 30, 2008; Revised Manuscript Received: June 11, 2008

To attempt theoretical predictions of the regioselectivity pattern in molecules with multiple reactive sites, the energies of formation of all possible isomers are usually considered. This means that the computing becomes highly demanding if high theoretical levels are used. The study objective was to predict the regioselectivity in the reaction of hydrogen addition onto azahydro[60]fullerene $C_{59}H_{n+1}N$ ($n = 0-4$) systems using a new reactivity indicator termed general-purpose reactivity indicator, $\Xi_{\Delta N \leq 0, \alpha}^k$, proposed by Anderson et al. (*J. Chem. Theory Comput.* **2007**, 3, 358). Because $\Xi_{\Delta N \leq 0, \alpha}^k$ combines the information from the electrostatic potential and the Fukui function, this indicator is a two-parameter model that depends on the atomic charges and Fukui values calculated. We used the gradient-corrected BLYP and BOP functionals to approximate the electronic density of the systems, and these densities were employed to determinate the parameters. In terms of regioselectivity, the preferential addition sites at every hydrogenation step on $C_{59}H_{n+1}N$ ($n = 0-4$) shows that 1,4-adducts are more stable than 1,2-adducts. However, we show that the multiple additions are only feasible up to a $C_{59}H_5N$ (tetraaddition) product. Consequently, the application of this indicator not only helps to avoid systematic computational studies by comparing energies of formation in several isomers—many of which are not currently supported by experimental results—but also provides an insight of how the pattern of addition is achieved. Comparisons with traditional indicators show that the application of $\Xi_{\Delta N \leq 0, \alpha}^k$ performs much better for predicting reactivity in the aza[60]fullerene derivatives studied.

1. Introduction

It is widely known that the reactivity of a chemical species also depends on its reactant counterpart. In particular, in fullerene chemistry, several studies¹⁻¹¹ have pointed out that by replacing one carbon atom for heteroatoms in the Bucky cage not only its structural properties but also its regioselectivity are changed. Although a rich variety of fullerene derivatives have been reported in the literature, the heterofullerenes¹⁻⁷ are of special interest in organic chemistry^{2,5} and material sciences^{6,7} because these compounds are expected to have applications in superconductivity, photoinduced electron transfer, and organic ferromagnetism.

Because of their unique electronic structure, fullerenes can undergo versatile chemical transformations, giving rise to a large number of complex and unusual derivatives. In comparison with neutral fullerenes, their respective aza derivatives⁸⁻¹¹ are among the most reactive relatives, since they have open-shell electronic configurations that increase their reactivity. In 1992, the simplest azafullerene was proposed to be the neutral $C_{59}N$ by Andreoni et al.,⁸ and only 3 years later, its experimental evidence was confirmed by Mattay and co-workers.⁹ Because of the presence of an unpaired electron in $C_{59}N$, two radical units can bind each other to form a closed-shell configuration, affording the diazafullerenyl ($C_{59}N$)₂ system.¹⁰ However, the attachment of hydrogen atoms onto the $C_{59}N$ cage can also readily lead to form closed-shell hydrogenated derivatives. The first computational study on azafullerenes¹¹ predicted that the binding

energies of the ($C_{59}N$)₂ dimer is ca. 18 kcal mol⁻¹; meanwhile, the respective binding energy for the hydrogenated $C_{59}HN$ derivative was estimated to be about 72 kcal mol⁻¹, thus suggesting that $C_{59}HN$ is the most stable closed-shell member of the aza[60]fullerenes family.

On the other hand, two decades ago, Parr and Yang^{12,13} rationalized the regioselectivity of organic reactions by applying the frontier molecular orbital (FMO) theory¹⁴ to local functions derived from density functional theory (DFT).^{15,16} As a result, one of the most important and fundamental tools in modern chemistry was proposed not only to deduce the hard-soft acid-base (HSAB) principle but also to provide information about chemical reactivity in any compound. This tool is the set of Fukui functions^{12,13} [e.g., $f^{(-)}(r)$, $f^{(0)}(r)$, and $f^{(+)}(r)$], which basically attributes the reactivity of a molecule with respect to electrophilic, radical, and nucleophilic attacks through linear responses of the electron density to charge transfer. Today, the Fukui function is an indicator extensively used for predicting relative site reactivities for many chemical systems (its logical motivation, interpretation, qualitative characteristics, and practical computation can be consulted elsewhere¹⁷). Moreover, the Fukui function has allowed for definitions of new chemical concepts, which had not been successfully defined in the FMO context but can be defined from the so-called “conceptual DFT” (e.g., local force fluctuations on nuclei, “universal” nucleofugality, etc.).^{16,18-21}

Because the evaluation of $f(r)$ is quite complicated, different procedures have been proposed. For instance, the Fukui function can be computed using two nonequivalent approaches, namely, the fragment of molecular response (FMR) or the response of molecular fragment (RMF).²² In particular, for a system of N

* To whom correspondence should be addressed. Tel: (52)55 56 22 47 39, ext. 224. E-mail: flavioc@nucleares.unam.mx.

[†] Centro de Ciencias Aplicadas y Desarrollo Tecnológico.

[‡] Instituto de Ciencias Nucleares.

electrons, Yang and Mortier²³ estimated the values of atomic condensed Fukui function, $f_{\alpha}^{(\pm)}(N)$ (often another level of abstraction is introduced), by computing independently the corresponding $(N - 1)$ -, N -, and $(N + 1)$ -electron systems with the same molecular geometry and using the MPA. The latter method corresponds to the FMR approach.

It is noteworthy that although Fukui's functions take into account orbital relaxation effects,^{24,25} this is only true for the condition where the early transition states are present. Hence, the phenomenon of larger Fukui values for higher reactivities is not applicable for all chemical systems. For example, Mendez and Gazquez^{26,27} and Li and Evans²⁸ have reported that the site of maximal Fukui function is not necessarily the most reactive place. Under these circumstances, it is worth verifying the validity of the concept and the application of these functions, for example, in fullerene-derived systems (e.g., aza[60]fullerenes) due to very scarce studies in this area.

Anderson et al.^{29,30} have recently derived a new reactivity indicator termed general-purpose, which is based on population analyses and on a dependence on the Fukui and the molecular electrostatic potentials as well (the Fukui potential is essential for describing reactions that are electron transfer-controlled, and the molecular electrostatic potential is essential for describing electrostatically controlled reactions). Thus, the new reactivity indicator, $\Xi_{\Delta N, \alpha}^{\kappa}$, represents a model for the interaction energies between any electrophile and any nucleophile and describes the local reactivity of molecules that lie between the electrostatic and the electron-transfer phenomena, including intermediate cases as well. The condensed forms of the indicator can be represented as follows:

$$\Xi_{\Delta N \leq 0, \alpha}^{\kappa} = (\kappa + 1)q_{\text{nucleophile}, \alpha}^{(0)} - \Delta N(\kappa - 1)f_{\text{nucleophile}, \alpha}^{(-)} \quad (1)$$

$$\Xi_{\Delta N \geq 0, \alpha}^{\kappa} = -(\kappa + 1)q_{\text{electrophile}, \alpha}^{(0)} + \Delta N(\kappa - 1)f_{\text{electrophile}, \alpha}^{(+)} \quad (2)$$

In these equations, the parameter κ controls the entire spectrum of chemical reactivity by modulating the electrostatic and Fukui function contributions to the interaction energy. In particular, values of $\kappa > 1$ describe a strong electrostatic control; $\kappa = 1$ describes a purely electrostatic control; $-1 < \kappa < 1$ describes a joint control by electrostatic and electron-transfer effects; $\kappa = -1$ describes a purely electron-transfer control; and values of $\kappa < -1$ describe a strong electron-transfer control. The value of $q_{\alpha}^{(0)}$ denotes the atomic charges on the electrophile or nucleophile reagents. $f_{\alpha}^{(+)}$ and $f_{\alpha}^{(-)}$ are the condensed Fukui functions of atom α in the reference system. Note that the $q_{\alpha}^{(0)}$ values are sensitive not only to the level of theory employed to compute the electron density but also to partition schemes. For example, because the Mulliken population analysis (MPA) is based on the one-particle density matrix defined over standard nonorthogonal atomic orbital basis set, then $q_{\alpha}^{(0)}$ will be sensitive to the selection of the basis set. As regards the values of ΔN , Anderson et al.^{29,30} have chosen the following convention: $\Delta N \leq 0$ for nucleophiles and $\Delta N \geq 0$ for electrophiles. Consequently, the smallest value of $\Xi_{\Delta N, \alpha}^{\kappa}$ is the most reactive atom.

Because of the fact that $C_{59}HN$ is a precursor of other aza derivatives by deprotonation and subsequent quenching of the anion with several electrophiles, the question of how well it preserves its reactivity is of special importance. Several works^{31–35} have theoretically analyzed the relative stability of different isomers of heterofullerenes but only at the semiempirical AM1 and MNDO levels of theory. Thus, Liang and co-workers^{31,32} have pointed out that the doping with heteroatoms strongly changes the patterns of regioselectivity in comparison with pristine C_{60} . In particular, the 1,2-adducts were identified as the most stable isomers of

aza[60]fullerenes followed by the 1,4-adducts. As it is well-known, C_{60} only reacts to give 1,2-adducts for the addition of pairs of hydrogen atoms.^{33–36}

In the present study, we focus on the regioselectivity of aza[60]fullerenes as well, but contrary to the study of Liang et al.³² where several computations were carried on to identify the most stable isomers, we have applied the newly proposed reactivity $\Xi_{\Delta N, \alpha}^{\kappa}$ indicator to predict the most possible positions of attack. Because the $C_{59}H_{n+1}N$ ($n = 0-4$) systems have multiple reactive sites, we have employed the reactivity transition tables proposed by Anderson et al.³⁰ to provide a useful way of showing how the most reactive sites change due to variations on the number of electrons (ΔN) and on the parameter κ . To make a reactivity transition table is necessary to compute the value of $\Xi_{\Delta N, \alpha}^{\kappa}$ (see eqs 1 and 2) for every atom in the molecule and for the entire chemically relevant range of choices for the amount of electron transfer and the extent of electrostatic/electron-transfer control.³⁰ In this fashion, these tables contain the smallest values calculated for $\Xi_{\Delta N, \alpha}^{\kappa}$, which correspond to the most reactive atoms in the molecular system. Thus, the reactivity $\Xi_{\Delta N}^{\kappa}$ indicator has been applied to study the pattern of hydrogen addition onto $C_{59}H_{n+1}N$ ($n = 0-4$) systems, and our results reveal that the multiple additions are only feasible up to a $C_{59}H_5N$ (tetraddition) product.

2. Theoretical Background

The electronic Fukui function, $f(r)$, can be interpreted either as the change of the electron density $\rho(r)$ at each point r when the total number of electrons is changed or as the sensitivity of a system's chemical potential to an external perturbation at a particular point r ,

$$f(r) = \left[\frac{\partial \rho(r)}{\partial N} \right]_v = \left[\frac{\delta \mu}{\delta v(r)} \right]_N \quad (3)$$

which is normalized, that is, $\int f(r) dr = 1$.

Because of the N -discontinuity problem of atoms and molecules,^{37–39} the introduction was necessary of both right- and left-hand side derivatives,¹² both to be considered at a given number of electrons, $N = N_0$:

$$f^{(+)}(r) = \left[\frac{\partial \rho(r)}{\partial N} \right]_{v(r)}^{+} \quad (4)$$

for a nucleophilic attack provoking an electron increase in the system and

$$f^{(-)}(r) = \left[\frac{\partial \rho(r)}{\partial N} \right]_{v(r)}^{-} \quad (5)$$

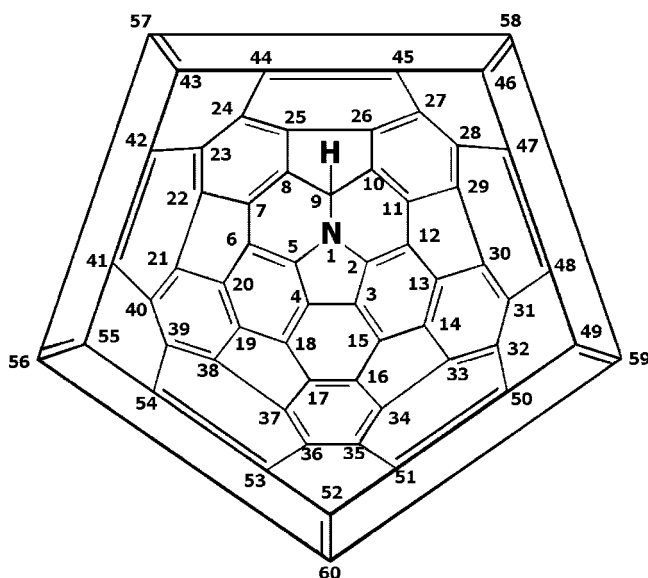
for an electrophilic attack provoking an electron decrease in the system. Recently, Ayers⁴⁰ carried on the differentiation of the energy function with respect to irrational numbers of electrons; the implications of that analysis were discussed on the response properties (e.g., Fukui function, electronegativity) used in the conceptual DFT.

In this fashion, the evaluation of expressions 4 and 5 is quite complicated. On the basis of the idea of integrating the Fukui functions over atomic regions with population analysis and combined with the finite difference approximation, Yang and Mortier²³ introduced the atomic condensed form of the Fukui function as follows:

$$f_{\alpha}^{(+)} = \tilde{q}_{\alpha}(N+1) - \tilde{q}_{\alpha}(N) \quad (6)$$

$$f_{\alpha}^{(-)} = \tilde{q}_{\alpha}(N) - \tilde{q}_{\alpha}(N-1) \quad (7)$$

where $\tilde{q}_{\alpha}(N)$ denotes the electronic population of atom α of the reference system.

SCHEME 1: Schlegel Diagram for Numbering of Atoms in the Azahydro[60]fullerene Systems


Because DFT is well-suited for the use with noninteger occupations, the analysis of the condensed Fukui functions can also be implemented by computing the finite differences according to the following expressions:

$$f_{\alpha}^{(+)} = [\tilde{q}_{\alpha}(N + \Delta N) - \tilde{q}_{\alpha}(N)] / \Delta N \quad (8)$$

$$f_{\alpha}^{(-)} = [\tilde{q}_{\alpha}(N) - \tilde{q}_{\alpha}(N - \Delta N)] / \Delta N \quad (9)$$

Thus, expressions 6 and 7 are a special case of eqs 8 and 9 with $\Delta N = 1$.

3. Computational Methods

The gradient-corrected functionals of Becke exchange⁴¹ and Lee–Yang–Parr correlation⁴² were used to approximate the electronic density of the $C_{59}H_{n+1}N$ ($n = 0-4$) systems. To see the effects on electron density by a change due to correlation effects, we have also tested possible variations employing the Tsuneda–Suzumura–Hirao⁴³ one-parameter progressive correlation functional (in conjunction with the Becke exchange; BOP for short). The basis set employed was a double numerical basis set with added polarization functions on all atoms (DNP).⁴⁴ This basis set includes as polarization functions a p-function on hydrogen and a d-function on carbon and nitrogen (all-electron treatment). Then, the calculated electronic densities are used to determine the values of the condensed Fukui functions. For all computations, we employed the DMol3 DFT software implemented in the Materials Studio Modeling 3.1 package from Accelrys, Inc.⁴⁵

A fine numerical integration grid (yielding more than 5000 points/atom) was employed. Convergence tolerance and orbital cutoff quality were set to fine, and global orbital cutoff (i.e., 3.7 Å) was employed as defined by the numerical basis set. We have recently tested this theoretical approach to study interactions in carbon nanotube-related systems,^{46,47} and we found that these methods are ideal in dealing with carbon derivatives. For the open-shell systems (e.g., $C_{59}H_2N$ and $C_{59}H_4N$), the computations were performed within the spin-unrestricted formalism. Vibrational frequencies were computed for all optimized structures to ensure that true minima were found. The numbering of the $C_{59}H_{n+1}N$ ($n = 0$) system (for a C_5 point of group symmetry) is shown in Scheme 1.

Finally, the values of $\Xi_{\Delta N, \alpha}^k$ (eqs 1 and 2) were computed employing the Fukui functions as expressed in eqs 8 and 9 (with $\Delta N = 0.1$).⁴⁸ Because the use of fractional charges for computing Fukui functions has not been well-established, in the present study, we only employed the value of 0.1 for ΔN in eqs 8 and 9. However, recently, it has been found⁴⁹ that the use of full electron treatment leads to errors of up to several hundred percent in the value of chemical potential as well as errors of about 5% in the atomic Fukui values. Although the current DMol3 version can control fractional values of ΔN , a clear advantage of using a value of $\Delta N = 0.1$ can be inferred just by monitoring the speed of SCF computations as well as the advance of SCF convergence.

4. Results and Discussion

The reactivity in molecular systems such as isoquinoline has been studied mainly within the frontier-orbital⁵⁰ and Fukui functions³⁰ frameworks. The Fukui function, $f_{\alpha}^{(-)}(r)$, will be larger at regions in the molecular system, which are minimally destabilized by removal of electrons; in other words, the Fukui function predicts that these regions [where $f_{\alpha}^{(-)}(r)$ is the largest] are susceptible to electrophilic attacks. However, using the reactivity indicator, $\Xi_{\Delta N}^k$, Anderson and co-workers^{30,51} studied the reactivity in isoquinoline³⁰ as well as in ambidentate nucleophiles and electrophiles.⁵¹ The authors employed the B3LYP/6-31G(d) level of theory to achieve a local minimum and then derived atomic charges from two different groups, namely, from methods that partitioned the density matrix [e.g., MPA⁵² and natural population analysis (NPA)⁵³] and methods for fitting the electrostatic potential (e.g., Merz–Singh–Kollman^{54,55} and ChelpG, CHG⁵⁶). Thus, the authors were able to explain the experimental regioselectivity on isoquinoline without too much difficulty,³⁰ and the application of $\Xi_{\Delta N}^k$ in ambidentate molecules was very useful.⁵¹ Because our BLYP/DNP computations use a unique approach to electrostatics and integration points generated in a spherical pattern around each atomic center, we decided to first test the reactivity also in isoquinoline but using the atomic charges derived from the MPA⁵² and Hirshfield⁵⁷ partitioning techniques as these are implemented in the DMol3 module.

4.1. Isoquinoline. The Fukui function, $f_{\alpha}^{(-)}$, and the reactivity indicator, $\Xi_{\Delta N, \alpha}^k$, were analyzed and compared to verify their reliability to predict the regioselectivity in neutral isoquinoline. We use the gradient-corrected BLYP functional to approximate the electronic density of isoquinoline, so that these densities were employed to compute the values of $f_{\alpha}^{(-)}$ and $\Xi_{\Delta N, \alpha}^k$. As a whole, no changes in the general trend are observed when we employ the BOP functional. As it is well-known, the Fukui function predicts that electrophilic reaction occurs where $f_{\alpha}^{(-)}$ is the largest. By using Mulliken charges in eq 9, we found that carbon 5 would be the most reactive site [$f_{C5}^{(-)} = 0.066$]. However, by using the Hirshfield charges, we found that the most reactive site is predicted to be carbon 3 [$f_{C3}^{(-)} = 0.093$]. Experimentally, Dewar and Maitlis⁵⁰ showed that the most reactive site is carbon 5, with a second reactive site at carbon 8 (carbon 4 is unreactive). Thus, we observe a concordance between the Fukui values that were derived from Mulliken charges and the experimental evidence; however, we note that these values cannot correctly predict the whole reactivity order as observed experimentally. For example, carbon 1 and nitrogen atom were predicted to be the places with the second highest reactivity, so that the reactivity order as calculated with MPA (i.e., Mulliken charges) follows the sequence: $C5 > C1 (=N) > C3$. With respect to the Fukui values derived from Hirshfield

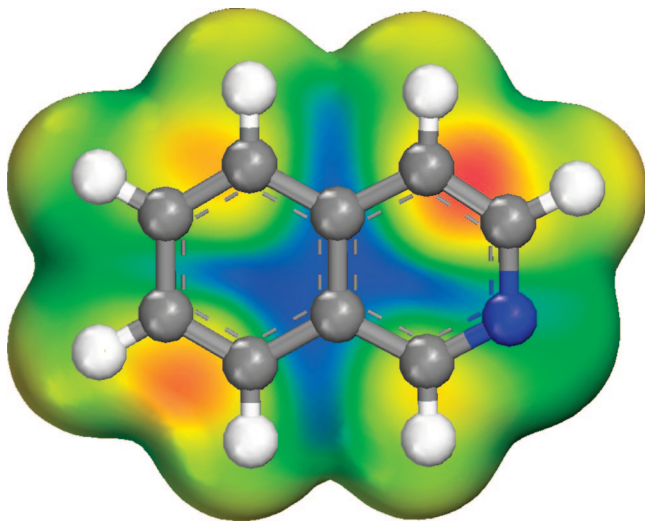


Figure 1. Fukui function, $f_{\alpha}^{(-)}(r)$, plotted over an isodensity of the isoquinoline molecule (at 0.017 au) as calculated at the BLYP/DNP level of theory.

scheme, these also fail to predict the reactivity order. In particular, carbon 4 (unreactive) and carbon 5 (the most reactive) turned out to be equally the second reactive sites [$f_{C4,C5}^{(-)} = 0.091$]; meanwhile, carbon 8 (the second reactive site) was computed as the third reactive site [$f_{C8}^{(-)} = 0.087$]. The reactivity order as calculated with Hirshfeld scheme follows the sequence: $C3 > C5 (=C4) > C8$. These results suggest that the Fukui function cannot predict the observed reactivity in isoquinoline. Figure 1 shows $f_{\alpha}^{(-)}(r)$ plotted over the isodensity of isoquinoline (Hirshfeld charges were employed). We can see that carbon 4 is slightly larger than that of carbon 8 (red zones), in concordance with the previous report of Anderson et al.³⁰ The van der Waals surface of isoquinoline was modeled with an isodensity surface at $\rho(r) = 0.017$ au. Because this surface encloses good enough the van der Waals volumes of the individual atoms, giving a good representation of the properties computed, we have also employed this value (i.e., 0.017 au) to model the respective van der Waals surface for all $C_{59}H_{n+1}N$ ($n = 0-4$) systems (see Figures 2).

With respect to $\Xi_{\Delta N, \alpha}^{\kappa}$, we found that carbon 5 is the most reactive for both MPA ($\Xi_{\Delta N=-1, C5}^{\kappa=-1} = -0.128$) and Hirshfeld ($\Xi_{\Delta N=-1, C5}^{\kappa=-1} = -0.186$) cases. This means that $\Xi_{\Delta N, \alpha}^{\kappa}$, which combines information from the electrostatic potential and the Fukui function, corrects the predicted reactivity as calculated with $f_{\alpha}^{(-)}(r)$. Unfortunately, $\Xi_{\Delta N, \alpha}^{\kappa}$ is unable to correct the reactivity order. According to Anderson et al.,³⁰ adding a proton to isoquinoline (i.e., under experimental conditions, isoquinoline forms ion-paired systems) leads to predictions into agreement with the experimental results. Because our goal was to predict the regioselectivity in neutral $C_{59}H_{n+1}N$ ($n = 0-4$) systems, we did not consider the case of ion-paired isoquinoline systems.

Several studies⁵⁷⁻⁶⁵ have shown that the Hirshfeld partitioning technique is significantly less basis set-dependent than most other population analysis techniques such as MPA, NBO, or molecular electrostatic potential (MESP)-based methods. For instance, Roy and co-workers⁶³⁻⁶⁵ have demonstrated (at the BLYP/DNP level of theory^{63,64} and within the finite difference scheme including $\Delta N = 1$) that the use of the Hirshfeld partitioning scheme can avoid negative condensed Fukui function values, thus solving the problem of interpreting the physical sense of these indices. Ayers et al.⁶⁵ also demonstrated that the condensed Fukui functions $f_{\alpha}^{(\pm)}(N)$ are generally more reliable reactivity indicators than the local Fukui functions $f_{\alpha}^{(\pm)}(r)$.

In this fashion, we have employed the Hirshfeld partitioning technique as a valuable tool to calculate reliable f_{α} values as indicated in eq 9. Thus, in the following subsections, we apply the charges derived from the Hirshfeld scheme to $\Xi_{\Delta N, \alpha}^{\kappa}$ (as indicated in eq 1) to predict the regioselectivity in neutral $C_{59}H_{n+1}N$ ($n = 0-4$) systems.

4.2. $C_{59}HN$ System. The main property of pristine C_{60} is its high electrophilicity, which made possible the synthesis of many derivatives via reductive chemical or electrochemical processes as well as through addition of nucleophiles; thus, it seems plausible that the indicator $\Xi_{\Delta N, \alpha}^{\kappa}$ will locate the appropriate sites for a nucleophilic attack on C_{60} -related compounds. However, the parent fullerene C_{60} undergoes electrophilic addition as well; this characteristic reaction of C_{60} takes place at 6,6-double bonds. To afford information about the addition regioselectivity onto $C_{59}HN$, the reactivity transition tables were compiled similar to those reported by Anderson et al.³⁰ These tables provide data on reactivity: At a quantitative level, they describe the relative favorability of the primary and secondary products, whereas at a qualitative level, the tables characterize the phase diagram for chemical reactivity. Tables 1, 2, 4, and 5 report the $\Xi_{\Delta N \leq 0, \alpha}^{\kappa}$ values (according to eq 1) for all $C_{59}H_{n+1}N$ ($n = 0-4$) systems, which all act as nucleophiles (i.e., $\Delta N \leq 0$). Thus, we employed the range $-1 \leq \Delta N \leq 0$ with an interval of $\Delta N = 0.1$; meanwhile, in the range $-1 \leq \kappa \leq 1$, two units have been used for the intervals of κ .

In Table 1, the $\Xi_{\Delta N \leq 0, \alpha}^{\kappa}$ values were determined considering that the $C_{59}HN$ system acts as a nucleophile and the reaction proceeds through an attack of a very strong electrophile (e.g., H^+), so that an isomer of $C_{59}H_2N$ will be formed. The goal of this section is provide information to help ensure which atom specific will react with the electrophile. The specific identity of the electrophile is not critical, however, so that it has been replaced with a model perturbation in the method for deriving the equations.^{66,67} Thus, in the beginning of the reaction, which can be mostly electron transfer-controlled ($\kappa \approx -1$), it appears that carbon 6 and carbon 12 (equivalent atoms in symmetry C_5) are the most reactive places. The respective values for these atoms are in blues boxes in Table 1a, where the values of $\Xi_{\Delta N \leq 0, \alpha}^{\kappa}$ denote the first choice of where the molecule is most reactive. Our results are in concordance with the previous AM1 study,³² which determined that the most energy-favored adduct is the one with carbon 6 as the first added site. In Table 1a, the parameter κ comprises the entire spectrum of chemical reactivity from $\kappa = -1$ (electron-transfer control) to $\kappa = 1$ (electrostatic control). As shown, the regioselectivity at C6/C12 atoms is preserved only up to a value of $\kappa = -0.4$ where a combination of electrostatic and electron transfer results in the maximum amount of charge transferred of 0.7e. This means that if the electrophile becomes softer and electrostatic interactions appear (i.e., $\kappa \geq 0$) then the nitrogen atom would be the preferred reaction site. In this case (i.e., $\kappa \approx 1$), the classical Coulombic interactions of the occupied orbitals of both reagents will control the addition of electrophilic reagent on nitrogen; nevertheless, this bonding has not been experimentally or theoretically reported. For this reason, we also considered the second most reactive atom, which is the atom that has the second smallest value for $\Xi_{\Delta N \leq 0, \alpha}^{\kappa}$. In this fashion, we have summarized in Table 1b the values of $\Xi_{\Delta N \leq 0, \alpha}^{\kappa}$ for the atom, which is the second choice (yellow boxes). We can see that the differences between the values of $\Xi_{\Delta N \leq 0, \alpha}^{\kappa}$ for the first choice (i.e., C6/C12) and the second choice (i.e., C25) are relatively large; thus, we expect that the addition of H^+ onto $C_{59}HN$ can only occur at C6/C12.

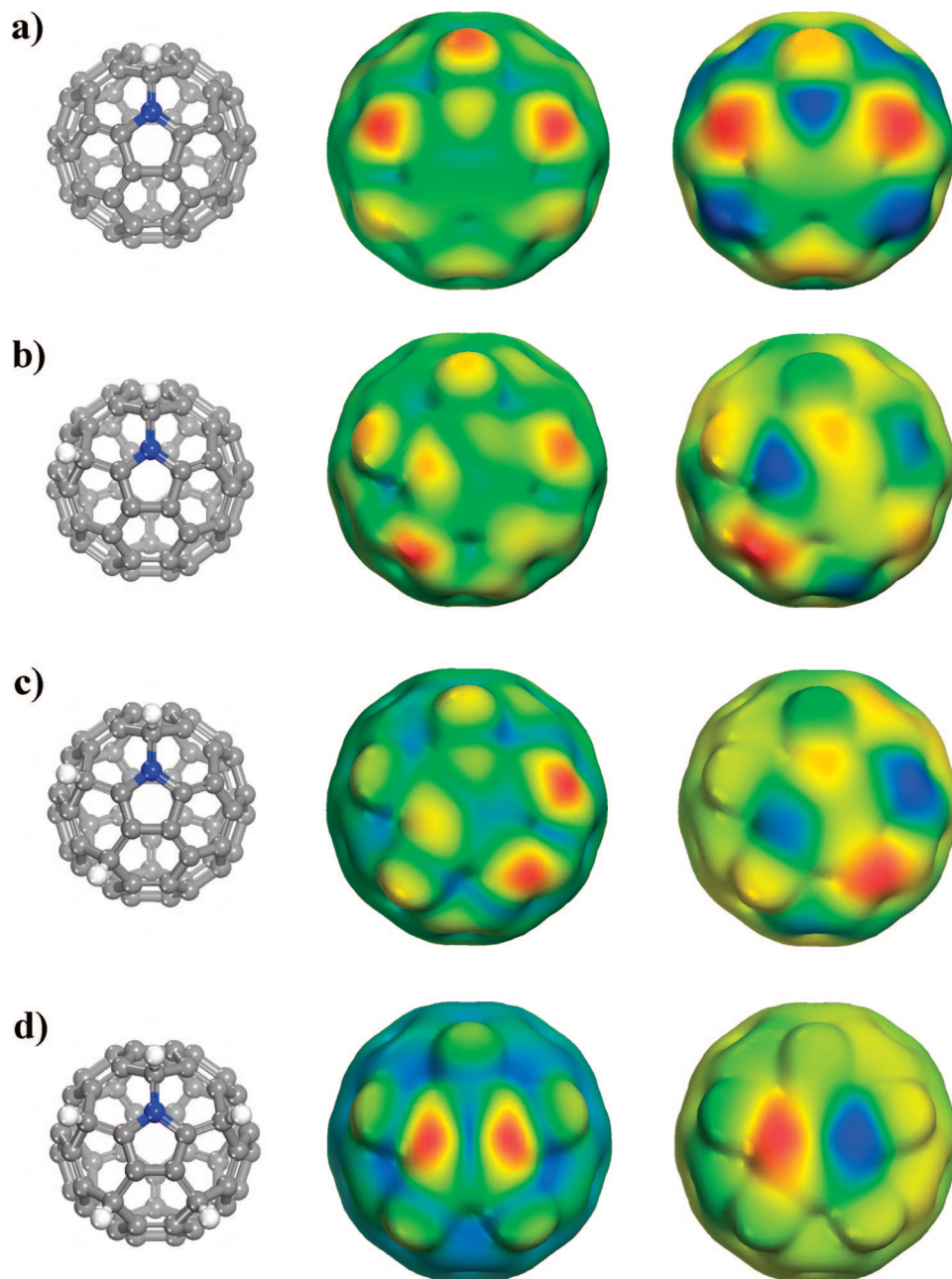


Figure 2. Optimized structures (left) at the BLYP/DNP level of theory and isodensities plotted (at 0.017 au) over $f^{(-)}(r)$ (center) and HOMO (right) functions for the $C_{59}H_{n+1}N$ ($n = 0-4$) systems.

As explained, larger f_{α} values at a site favor reactivity at that site. However, in the frozen core approximation, the FMO theory¹⁴ is equivalent to the assumption that it is favorable for f_{α} to be large at a site, where the incoming reagent will produce the biggest change in the system [e.g., $f^{(-)}(r) \approx \rho_{\text{HOMO}}(r)$]. Figure 2 shows the isodensities for $C_{59}H_{n+1}N$ ($n = 0-4$) systems plotted (at 0.017 au) over $f^{(-)}(r)$ and the highest occupied molecular orbital (HOMO), center and right, respectively. The preferred sites governing electrophilic attacks are localized in the red zones. For the case of $C_{59}HN$ (Figure 2a), on one hand, we can see that the largest $f^{(-)}(r)$ values are localized not only at C6/C12 atoms but also at the hydrogen position. On the other hand, the HOMO isosurface (right) shows that the reactivity is localized only at C6/C12 atoms. Meanwhile, the corresponding Fukui values (computed using the Hirshfeld scheme) for C6/C12 and H atoms are $f_{\text{C6/C12}}^{(-)} = 0.038$ and $f_{\text{H}}^{(-)} = 0.023$, respectively, and the computed charge for H atom is a positive

value ($q_{\text{H}}^{\text{Hirshfeld}} = 0.043$). This result shows the inadequacy of the well-known frontier-controlled vs charge-controlled dichotomy for describing regioselectivity in aza[60]fullerene systems. More detailed examples where orbital relaxation is an important contribution to the Fukui functions can be found elsewhere.^{24,25,68}

As previously mentioned, using the $\Xi_{\Delta N \leq 0, \alpha}^{\kappa}$ indicator, the reactivity in $C_{59}HN$ is predicted to be equitably at C6/C12 atoms, and the reason that explains why these atoms are susceptible to electrophilic additions can be explained in terms of resonance. Because the lone pair of electrons on nitrogen atom is conjugated with two double bonds localized on the C6—C5 and C2—C12 atoms, some degree of delocalization is observed in the system. In this way, electrophiles react with the unshared electrons temporally localized on C6/C12 atoms, which behave as carbanions. According to Hirshfeld and MPA schemes, the lowest charges are localized on C6 and C12 atoms, and the

TABLE 1: Reactivity Transition Tables (Part a, First Choice; Part b, Second Choice) Calculated for the $C_{59}H_{n+1}N$ ($n = 0$) System as a Nucleophile and Using the Hirshfield Scheme in the Population Analysis

(a)

	κ										
ΔN	1.0	0.8	0.6	0.4	0.2	0	-0.2	-0.4	-0.6	-0.8	-1.0
-1.0	-0.073	-0.072	-0.070	-0.069	-0.068	-0.066	-0.065	-0.067	-0.070	-0.073	-0.076
-0.9	-0.073	-0.071	-0.069	-0.067	-0.065	-0.063	-0.062	-0.062	-0.064	-0.066	-0.068
-0.8	-0.073	-0.070	-0.068	-0.065	-0.063	-0.060	-0.058	-0.056	-0.058	-0.059	-0.061
-0.7	-0.073	-0.070	-0.067	-0.064	-0.060	-0.057	-0.054	-0.051	-0.052	-0.052	-0.053
-0.6	-0.073	-0.069	-0.065	-0.062	-0.058	-0.054	-0.051	-0.047	-0.046	-0.046	-0.046
-0.5	-0.073	-0.069	-0.064	-0.060	-0.056	-0.051	-0.047	-0.043	-0.040	-0.039	-0.038
-0.4	-0.073	-0.068	-0.063	-0.058	-0.053	-0.048	-0.044	-0.039	-0.033	-0.032	-0.030
-0.3	-0.073	-0.067	-0.062	-0.056	-0.051	-0.045	-0.040	-0.034	-0.029	-0.025	-0.023
-0.2	-0.073	-0.067	-0.061	-0.055	-0.048	-0.042	-0.036	-0.030	-0.024	-0.018	-0.015
-0.1	-0.073	-0.066	-0.059	-0.053	-0.046	-0.039	-0.033	-0.026	-0.019	-0.011	-0.008
0.0	-0.073	-0.066	-0.058	-0.051	-0.044	-0.036	-0.029	-0.022	-0.015	-0.007	
Nitrogen						Carbon 6 (= Carbon 12)					

(b)

	κ										
ΔN	1.0	0.8	0.6	0.4	0.2	0	-0.2	-0.4	-0.6	-0.8	-1.0
-1.0	-0.024	-0.026	-0.029	-0.032	-0.034	-0.037	-0.039	-0.042	-0.045	-0.047	-0.050
-0.9	-0.024	-0.026	-0.028	-0.030	-0.032	-0.034	-0.036	-0.039	-0.041	-0.043	-0.045
-0.8	-0.024	-0.025	-0.027	-0.029	-0.030	-0.032	-0.033	-0.035	-0.037	-0.038	-0.040
-0.7	-0.024	-0.025	-0.026	-0.027	-0.028	-0.029	-0.030	-0.032	-0.033	-0.034	-0.035
-0.6	-0.024	-0.024	-0.025	-0.026	-0.026	-0.027	-0.027	-0.028	-0.029	-0.029	-0.030
-0.5	-0.024	-0.024	-0.024	-0.024	-0.024	-0.024	-0.024	-0.025	-0.025	-0.025	-0.025
-0.4	-0.024	-0.023	-0.023	-0.023	-0.022	-0.022	-0.021	-0.021	-0.021	-0.020	-0.020
-0.3	-0.024	-0.023	-0.022	-0.021	-0.020	-0.019	-0.018	-0.018	-0.017	-0.016	-0.015
-0.2	-0.024	-0.022	-0.021	-0.020	-0.018	-0.017	-0.015	-0.014	-0.013	-0.011	-0.010
-0.1	-0.024	-0.022	-0.020	-0.018	-0.016	-0.014	-0.012	-0.011	-0.009	-0.007	-0.005
0.0	-0.024	-0.021	-0.019	-0.017	-0.014	-0.012	-0.009	-0.007	-0.005	-0.002	
Carbon 25											

TABLE 2: Reactivity Transition Table Calculated for $C_{59}H_{n+1}N$ ($n = 1$) as the Nucleophile and Using the Hirshfield Scheme in the Population Analysis

	κ										
ΔN	1.0	0.8	0.6	0.4	0.2	0	-0.2	-0.4	-0.6	-0.8	-1.0
-1.0	-0.055	-0.053	-0.051	-0.049	-0.048	-0.051	-0.054	-0.057	-0.060	-0.066	-0.072
-0.9	-0.055	-0.053	-0.050	-0.048	-0.045	-0.047	-0.050	-0.052	-0.054	-0.060	-0.065
-0.8	-0.055	-0.052	-0.049	-0.047	-0.044	-0.044	-0.046	-0.048	-0.049	-0.053	-0.058
-0.7	-0.055	-0.052	-0.049	-0.046	-0.043	-0.041	-0.042	-0.043	-0.044	-0.047	-0.050
-0.6	-0.055	-0.052	-0.048	-0.045	-0.041	-0.038	-0.038	-0.038	-0.038	-0.040	-0.043
-0.5	-0.055	-0.051	-0.047	-0.044	-0.040	-0.036	-0.034	-0.034	-0.032	-0.034	-0.036
-0.4	-0.055	-0.051	-0.047	-0.043	-0.038	-0.034	-0.030	-0.029	-0.027	-0.027	-0.029
-0.3	-0.055	-0.051	-0.046	-0.042	-0.037	-0.033	-0.028	-0.024	-0.023	-0.021	-0.022
-0.2	-0.055	-0.050	-0.045	-0.041	-0.036	-0.031	-0.026	-0.020	-0.018	-0.014	-0.014
-0.1	-0.055	-0.050	-0.045	-0.040	-0.034	-0.029	-0.024	-0.019	-0.012	-0.008	-0.007
0.0	-0.055	-0.050	-0.044	-0.038	-0.033	-0.028	-0.022	-0.016	-0.007	-0.004	
Carbon 4				Carbon 12				Carbon 18			

computed charges on these atoms are $q_{C6,C12}^{Hirshfield} = -0.023$ and $q_{C6,C12}^{Mulliken} = -0.034$, respectively. In this fashion, our results confirm the reliability of $\Xi_{\Delta N \leq 0, \alpha}^{\kappa}$ indicator for predicting the reactivity in the $C_{59}HN$ system.

4.3. $C_{59}H_2N$ System. As regards $C_{59}H_2N$ (where the second hydrogen was positioned on carbon 6), this system was not considered by Liang et al.³² However, on the basis of the calculations for the heats of formation of $C_{59}H_3N$, the authors predicted that 1,2-adducts are more stable than 1,4-adducts except for 6,18-isomer. Table 2 shows the $\Xi_{\Delta N \leq 0, \alpha}^{\kappa}$ values for the $C_{59}H_2N$ system, where it acts as a nucleophile and the reaction will proceed to form $C_{59}H_3N$. In this fashion, to form the most energy-favored adduct, we expected that the smallest $\Xi_{\Delta N \leq 0, \alpha}^{\kappa}$ values are for a particular carbon, which leads to form any 1,4-adduct. In fact, according to the values shown in Table 2 (blue boxes), the most reactive site for an electrophilic attack is mainly localized at carbon 18; thus, the isomer 6,18-isomer is formed. We can see that the regioselectivity of carbon 18 is

TABLE 3: Electronic Energies for the $C_{59}H_{n+1}N$ ($n = 2-4$) Systems as Calculated at the BLYP/DNP and BOP/DNP Levels of Theory

isomer	adduct	ΔE (kcal mol ⁻¹)			
		BLYP	$\Delta \Delta E^c$	BOP	$\Delta \Delta E^c$
6,18 ^a	1,4	-18.58		-16.52	
16,17	1,2	-17.36	1.2	-15.60	0.9
21,40 ^b	1,2	-16.92	1.7	-14.85	1.7
6,18/15	1,4/1	-24.20		-22.15	
6,18/12	1,4/1	-21.01	3.2	-18.95	3.2
6,18/12,15	1,4/1,4	-26.82		-24.99	
6,18/3,15	1,4/1,2	-12.78	14.0	-10.72	14.3

^a Equivalent to the 12,15-isomer. ^b Equivalent to the 30,31-isomer. ^c Difference between the isomers and the most energetically stable structure.

dominant up to a value of $\kappa = -0.6$, which is a condition for reacting through electron transfer (i.e., $\Delta N = -0.4$). This

TABLE 4: Reactivity Transition Table Calculated for $C_{59}H_{n+1}N$ ($n = 2$) as the Nucleophile Using the Hirshfield Scheme in the Population Analysis

	K										
ΔN	1.0	0.8	0.6	0.4	0.2	0	-0.2	-0.4	-0.6	-0.8	-1.0
-1.0	-0.071	-0.070	-0.069	-0.069	-0.068	-0.067	-0.070	-0.075	-0.080	-0.085	-0.092
-0.9	-0.071	-0.069	-0.068	-0.067	-0.066	-0.064	-0.065	-0.069	-0.073	-0.077	-0.081
-0.8	-0.071	-0.069	-0.067	-0.065	-0.063	-0.061	-0.059	-0.062	-0.066	-0.069	-0.074
-0.7	-0.071	-0.068	-0.066	-0.063	-0.060	-0.058	-0.055	-0.056	-0.058	-0.061	-0.064
-0.6	-0.071	-0.068	-0.064	-0.061	-0.058	-0.055	-0.051	-0.050	-0.051	-0.053	-0.055
-0.5	-0.071	-0.067	-0.063	-0.059	-0.055	-0.051	-0.048	-0.044	-0.044	-0.045	-0.046
-0.4	-0.071	-0.066	-0.062	-0.057	-0.053	-0.048	-0.044	-0.039	-0.037	-0.036	-0.037
-0.3	-0.071	-0.066	-0.060	-0.055	-0.050	-0.045	-0.040	-0.035	-0.030	-0.028	-0.028
-0.2	-0.071	-0.065	-0.059	-0.053	-0.048	-0.042	-0.036	-0.030	-0.022	-0.020	-0.018
-0.1	-0.071	-0.064	-0.058	-0.051	-0.045	-0.039	-0.032	-0.026	-0.015	-0.012	-0.009
0.0	-0.071	-0.064	-0.057	-0.050	-0.042	-0.035	-0.028	-0.021	-0.008	-0.004	
Carbon 4				Carbon 12				Carbon 15			

TABLE 5: Reactivity Transition Table Calculated for $C_{59}H_{n+1}N$ ($n = 3$) as the Nucleophile Using the Hirshfield Scheme in the Population Analysis

	K										
ΔN	1.0	0.8	0.6	0.4	0.2	0	-0.2	-0.4	-0.6	-0.8	-1.0
-1.0	-0.089	-0.089	-0.089	-0.088	-0.088	-0.088	-0.087	-0.101	-0.118	-0.135	-0.152
-0.9	-0.089	-0.088	-0.087	-0.086	-0.084	-0.083	-0.082	-0.090	-0.106	-0.121	-0.137
-0.8	-0.089	-0.087	-0.085	-0.083	-0.081	-0.079	-0.077	-0.080	-0.094	-0.108	-0.122
-0.7	-0.089	-0.086	-0.083	-0.080	-0.078	-0.075	-0.072	-0.069	-0.082	-0.094	-0.106
-0.6	-0.089	-0.085	-0.082	-0.078	-0.074	-0.070	-0.067	-0.063	-0.069	-0.080	-0.091
-0.5	-0.089	-0.085	-0.080	-0.075	-0.071	-0.066	-0.061	-0.057	-0.057	-0.067	-0.076
-0.4	-0.089	-0.084	-0.078	-0.073	-0.067	-0.062	-0.056	-0.051	-0.045	-0.053	-0.061
-0.3	-0.089	-0.083	-0.077	-0.070	-0.064	-0.058	-0.051	-0.045	-0.038	-0.039	-0.046
-0.2	-0.089	-0.082	-0.075	-0.068	-0.060	-0.053	-0.046	-0.039	-0.032	-0.026	-0.030
-0.1	-0.089	-0.081	-0.073	-0.065	-0.057	-0.049	-0.041	-0.033	-0.025	-0.017	-0.015
0.0	-0.089	-0.080	-0.071	-0.062	-0.054	-0.045	-0.036	-0.027	-0.018	-0.009	
Carbon 4 (= Carbon 3)								Carbon 5 (= Carbon 2)			

observation is consistent with the Fukui index computed [$f_{C18}^{(-)} = 0.036$], which is the largest value found. The red boxes show the values for $\Xi_{\Delta N \leq 0, \alpha}^K$ that corresponds to carbon 12, which has the smallest values for $\Xi_{\Delta N \leq 0, \alpha}^K$ at $0 \leq \kappa \leq -0.4$. As we can see, the reactivity for this atom is a combination of electrostatic and charge transfer factors; this means that if the electrophile is not strong enough, the reaction can occur preferentially at this site. These results suggest that the electrophilic substitution on $C_{59}H_2N$ can lead to two isomers provided that the reagent is not sufficiently hard. For example, because the partial charge at carbon 18 is neutral ($q_{C18}^{\text{Hirshfield}} = -0.001$), the resonance between the charges of carbon 5 ($q_{C5}^{\text{Hirshfield}} = 0.049$), the lone pair on N ($q_N^{\text{Hirshfield}} = -0.017$), and carbon 12 ($q_{C12}^{\text{Hirshfield}} = -0.018$) allows for the charge on carbon 12 to be temporarily positive; thus, this atom can react with the reagent. The Fukui indexes computed for carbons 12 and 5 are $f_{C12}^{(-)} = 0.033$ and $f_{C5}^{(-)} = 0.028$, respectively. In Figure 2b are shown (in red color) the zones governing electrophilic attack. As in the case of $C_{59}HN$, we plotted its isodensity over the computed $f^{(-)}(r)$ and HOMO functions. We can see that both isodensities are different due to the fact that basically two reactive sites appear with $f^{(-)}(r)$ and only one site with HOMO. This result shows, on one hand, that the dichotomy of an equivalent assumption for $f^{(-)}(r) \approx \rho_{\text{HOMO}}(r)$ is not applicable in aza[60]fullerenes and, on the other hand, the validity of the $\Xi_{\Delta N \leq 0, \alpha}^K$ indicator for predicting reactivity in molecules with multiple reactive sites. Finally, in comparison with $C_{59}HN$ where the nitrogen atom is the most reactive one at $\kappa \approx 1$ conditions, for the $C_{59}H_2N$ molecule, it appears that carbon 4 is the preferential site (i.e., $\Xi_{\Delta N \leq 0, C4}^{\kappa=1} = -0.055$).

4.4. $C_{59}H_3N$ System. The next reaction step considered is the addition of hydrogen onto $C_{59}H_2N$ to form $C_{59}H_3N$. According to the energies of formation calculated by Liang et al.³² at the levels AM1 and MNDO, the $C_{59}H_3N$ system has

several isoenergetic isomers. The authors studied 16 possible 1,2-adducts and 30 possible 1,4-adducts of pairs of hydrogen atoms onto $C_{59}HN$ and found that the 6,18-isomer is the energetically most favored adduct with respect to the second (16,17-) and third (21,40-) isomers in ca. 3.5 kcal mol⁻¹. To verify this result, we studied at the BLYP/DNP and BOP/DNP levels of theory only the three most stable isomers of $C_{59}H_{n+1}N$ ($n = 2$) as previously predicted by the AM1 and MNDO methods. In Table 3, we report the respective electronic energies of the isomers as calculated at the GGA-DFT methods listed above (for numbering, see Scheme 1). As a whole, the 6,18-isomer ($\Delta E^{\text{BLYP}} = -18.6$ kcal mol⁻¹), which is the 1,4-adduct, is more stable than 1,2-adducts in ca. 1.5 kcal mol⁻¹ (see the differences between the isomers and the most energetically stable structure, $\Delta\Delta E$, in Table 3). Thus, the stability of 6,18-isomer with respect to the 16,17-isomer ($\Delta E^{\text{BLYP}} = -17.4$ kcal mol⁻¹) is higher by ca. 1.2 kcal mol⁻¹, and with respect to the 21,40-isomer ($\Delta E^{\text{BLYP}} = -16.9$ kcal mol⁻¹), it is higher by ca. 1.7 kcal mol⁻¹. Clearly, the difference of ca. 1 kcal mol⁻¹ with respect to the values reported by Liang et al.³² is due to the levels of theory employed. Finally, computing their harmonic normal modes of vibration assessed the structural stability and feasibility of 6,18-, 16,17-, and 21,40-isomers. The lowest-lying normal vibration for each of the isomers was found to be at 227, 223, and 221 cm⁻¹, respectively. The absence of imaginary frequencies indicates that all of the optimized structures are truly local minima.

Starting from $C_{59}H_3N$, it is possible to obtain 77 possible adducts (27 and 50 isomers, respectively, for 1,2- and 1,4-adducts) for $C_{59}H_5N$. The situation becomes most complicated if we want to know which is the most stable isomer for $C_{59}H_4N$ as well as $C_{59}H_5N$ systems. Moreover, if we assume a further addition to $C_{59}H_3N$, then a total of 38 isomers of $C_{59}H_7N$ are possible to obtain. Thus, it is clear that the computing becomes

highly demanding if high theoretical levels are used. In this way, rather than to study all possible isomers (e.g., 46 isomers for $C_{59}H_3N$), we applied the $\Xi_{\Delta N \leq 0, \alpha}^{\kappa}$ indicator to attempt a theoretical prediction of the regioselectivity in $C_{59}H_3N$.

The $\Xi_{\Delta N \leq 0, \alpha}^{\kappa}$ values calculated for the 6,18-isomer of $C_{59}H_3N$ are shown in Table 4. We can see that the electrophilic attack is favored at carbon 15 through a pure electron-transfer regime (i.e., $\kappa = -1$). Meanwhile, the combination of charge transfer with a little contribution of electrostatic makes possible that the reaction will occur at carbon 12. The $\Xi_{\Delta N \leq 0, \alpha}^{\kappa}$ values calculated for C15 and C12 are shown in the blue and red boxes, respectively. As for the $C_{59}H_2N$ case, we observed that carbon 4 is the most reactive site for reacting through a pure electrostatic control (see values in the white boxes). Figure 2c shows the isodensity plotted over the computed $f^{(-)}(r)$ and HOMO functions for the 6,18-isomer of $C_{59}H_3N$. On one hand, according to the isosurface plotted over $f^{(-)}(r)$ (center), it appears that not only carbon 15 is a reactive site but also carbon 12 (see red zones). On the other hand, according to the HOMO isosurface (right), we see that only carbon 15 is a reactive site in the molecule. The question whether Kohn–Sham orbitals¹⁵ have a physical meaning was extensively discussed elsewhere (see, for example, ref 69). The main limitation for predicting where a reaction will take place using FMO theory¹⁴ is that it validates the orbital model without incorporating electron correlation and orbital relaxation quantum effects. However, a different picture comes from the charge partitioning (by Hirshfeld scheme), which suggests that carbon 12 ($q_{C12}^{\text{Hirshfeld}} = -0.020$) is the reactive site to add electrophiles due to the fact that it is three times more negative than carbon 15 ($q_{C15}^{\text{Hirshfeld}} = -0.007$). Through a pure electron-transfer mechanism (i.e., $\kappa = -1$), the contribution of the $q_{\text{nucleophile}, \alpha}^{(0)}$ values into the first term of eq 1 is null, so that the equation can be reduced to $\Xi_{\Delta N \leq 0, \alpha}^{\kappa = -1} = 2\Delta N f_{\text{nucleophile}, \alpha}^{(-)}$. Because the Fukui potential is usually large at the same sites where the Fukui function is large, electron transfer-controlled reactions tend to occur where the Fukui function is large.²⁹ The Fukui indexes computed for carbon 15 and 12 are $f_{C15}^{(-)} = 0.046$ and $f_{C12}^{(-)} = 0.045$, respectively, which suggests that both atoms are almost equivalent for reacting with electrophiles, in concordance with the prediction of $\Xi_{\Delta N \leq 0, \alpha}^{\kappa}$ indicator. Thus, the Fukui functions developed by Parr and Yang^{12,13} in principle are far more valuable tools for predicting regioselectivity in the $C_{59}H_3N$ system at $\kappa = -1$.

4.5. $C_{59}H_4N$ and $C_{59}H_5N$ Systems. Because there is virtually no difference for the predicted reactivity on carbons 12 and 15, the hydrogen addition will lead to two possible isomers of $C_{59}H_4N$. To verify which of the isomers is most energetically preferred, we also computed their respective formation energies by using the expression $\Delta E = E_{C_{59}H_4N} - (E_{C_{59}H_2N} + E_{H_2})$. We found, at the BLYP/DNP level of theory, that there is a difference of ca. 3 kcal mol⁻¹ (at 0 K) between the isomers, 6,18/15-isomer being the most stable structure ($\Delta E^{\text{BLYP}} = -24.2$ kcal mol⁻¹). Likewise, at the BOP/DNP level of theory, the difference of energies between the isomers, $\Delta \Delta E$, is ca. 3 kcal mol⁻¹ (see Table 3). The mean absolute deviation for the BLYP and BOP methods for a set of molecules was calculated⁴³ to be ca. 3 kcal mol⁻¹; consequently, the 6,18/12- and 6,18/15-isomers can be considered as isoenergetic so that the addition can equally occur at both positions (i.e., C12/C15).

The next addition step on either the 6,18/12- or the 6,18/15-isomer leads to the formation of $C_{59}H_5N$ compounds. The experimental observation of $C_{59}H_5N$ was reported by Vasil'ev and co-workers.⁷⁰ The latter study suggests that increasing the degree of hydrogenation reduces electron affinity of azafullerenes,

so that the highest degree of hydrogenation is the one in $C_{59}H_5N$. The authors suggested that the lowest-energy structure for $C_{59}H_5N$ corresponds to 6,18/12,15-isomer. In addition, Reuther and Hirsch⁷¹ found in the chlorination of monoarylated azafullerenes that up to five addends occupy the 1-, 6-, 18-, 12-, and 15-positions, supporting the structure proposed in other studies.^{32,70} With respect to the theoretical studies, Liang et al.³² found at the levels AM1 and MNDO that 6,18/12,15-isomer (i.e., 1,4/1,4-adduct) of $C_{59}H_5N$ is more energetically stable than the second most stable 6,18/3,15-isomer (i.e., 1,4/1,2-adduct) by ca. 14 kcal mol⁻¹. To know the relative stability of the 6,18/12,15-isomer with respect to the 6,18/3,15-isomer, we calculated their electronic energies at the BLYP/DNP and BOP/DNP levels of theory (values shown in Table 3). Here, we can see that 6,18/12,15-isomer ($\Delta E^{\text{BLYP}} = -26.8$ kcal mol⁻¹) is more stable by ca. 14 kcal mol⁻¹ than 6,18/3,15-isomer ($\Delta E^{\text{BLYP}} = -12.8$ kcal mol⁻¹), a difference that agrees very well with the previously reported AM1 results.³² The high stability of the 6,18/12,15-isomer can be attributed to a high electronic density at its 6 π central pentagonal ring, which also suggests that this isomer is an aromatic compound.⁷⁰ According to our results, the optimized N–C bond lengths in this compound notably are shorter than the ones in $C_{59}HN$. For example, at the BLYP/DNP level of theory, the length of the C2–C3 and C4–C5 bonds is 1.384 Å; meanwhile, the length of the same bonds in $C_{59}HN$ is 1.441 Å. The lengths of N–C9, C2–C12 (C5–C6), and C3–C15 (C4–C18) bonds in $C_{59}H_5N$ are 1.491, 1.509, and 1.512 Å, respectively. Moreover, we found a planar configuration for the central pyrrole moiety (i.e., the dihedral angle $\angle N-C2-C3-C4$ is 0.0°), which is surrounded by the sp³ carbons 6, 12, 15, and 18. This result implies that the pentagonal ring in the center creates an aromatic five-membered pyrrolelike structure. The optimized geometry as well as the isodensity plotted in conjunction with the computed $f^{(-)}(r)$ (center) and HOMO (right) for the 6,18/12,15-isomer of $C_{59}H_5N$ are shown in Figure 2d.

As regards $\Xi_{\Delta N \leq 0, \alpha}^{\kappa}$ values calculated for the 6,18/12,15-isomer (values are shown in Table 5), we can see that apparently carbon 2 as well as carbon 5 would be the next reactive sites toward electrophiles. It is interesting to analyze the differences between the use of $\Xi_{\Delta N \leq 0, \alpha}^{\kappa}$ indicator^{29,30} and energetical-only considerations³² for predicting the regioselectivity in $C_{59}H_{n+1}N$ systems. According to the values shown in Table 5, the reactivity on C2/C5 is mainly due to an electron-transfer control; meanwhile, C3/C4 will be reactive only if an electrostatic control appears. The charge partitioning by Hirshfeld method considers that carbon 2 and carbon 5 are unreactive sites in the molecule. The charges, $q_{\alpha}^{\text{Hirshfeld}}$, on these atoms are 0.009 and -0.045, respectively. At the same time, we found that in $C_{59}H_5N$ both carbons 2 and 5 have the same highest Fukui indexes (i.e., $f_{C2/C5}^{(-)} = 0.076$). Moreover, the second highest values calculated for the Fukui indexes are for carbon 3 and carbon 4 (i.e., $f_{C3/C4}^{(-)} = 0.043$). On the basis of the energetical considerations proposed by Liang et al.,³² the authors concluded that the following next favorable structure from $C_{59}H_5N$ is the 6,18/12,15/44,45-isomer. However, according to the $\Xi_{\Delta N \leq 0, \alpha}^{\kappa}$ values calculated by us for carbons 44 and 45, we can see that these atoms are unreactive sites at both $\kappa = -1$ (electron-transfer) and $\kappa = 1$ (electrostatic) conditions. In particular, at the $\kappa = -1$, the values calculated for carbon 44 and carbon 45 are $\Xi_{\Delta N = -1, C44}^{\kappa = -1} = -0.030$ and $\Xi_{\Delta N = -1, C45}^{\kappa = -1} = -0.026$, respectively, which means that these atoms are about five times less reactive than carbon 2 and carbon 5.

From Figure 2d, it appears that no differences between the isodensities plotted with the $f^{(-)}(r)$ values and HOMO function are observed. This means that HOMO electron density (right), which is mainly localized on the C2–C3 and C4–C5 bonds, also predicts a localized regioselectivity for reacting with electrophiles at these sites. Experimentally, the formation of isomers higher than $C_{59}H_5N$ has not been reported, which can be explained by the formation of pyrrole nucleus in $C_{59}H_5N$ system, which provides a high stability for the structure. As it is well-known, the pyrrole molecule undergoes electrophilic aromatic substitution predominantly at C2/C5 atoms; therefore, we believe that further possible reactions of $C_{59}H_5N$ can be arylation or cycloadditions^{1,2,4} rather than the addition of H_2 . As an example, the covalent linking of $C_{59}H_5N$ with porphyrin derivatives upon thermal activation might be of a particular practical importance, since related systems exhibited long-lived intramolecular charge separation that can be applied in $C_{59}H_5N$ -based donor–acceptor photovoltaics ensembles.⁷²

Finally, we showed that the application of the general-purpose reactivity indicator helps to avoid tedious systematic analysis of possible addition sites in the systems studied (i.e., azahydro[60]-fullerene derivatives). Thus, the indicator $\Xi_{\Delta N, \alpha}^K$ helps to provide theoretical insights into the multiple addition onto $C_{59}H_{n+1}N$ ($n = 0-4$) systems without comparing formation energies for numerous possible isomers, which implies a significantly reduced computational time and human effort. We believe that this indicator is an effective reactivity tool and should be added to the toolbox of chemists working on reactivity. However, the theoretical description of chemical reactivity indicators (descriptors) is nowadays an active area of research (thanks mostly to Parr and Yang's^{12,13} papers); thus, it is certainly important to establish whether $\Xi_{\Delta N, \alpha}^K$ is indeed of “general purpose”.

5. Conclusions

In the present study, we attempt to give some insight of the regioselectivity in the azahydro[60]fullerene derivatives. In this fashion, the general-purpose reactivity indicator, $\Xi_{\Delta N \leq 0, \alpha}^K$, proposed by Anderson et al.²⁹ was applied to study electrophilic addition reaction of hydrogenation on $C_{59}H_{n+1}N$ ($n = 0-4$) systems. Thus, we predicted the preferential addition sites at every hydrogenation step. The values of $\Xi_{\Delta N \leq 0, \alpha}^K$ indicator were derived from the Fukui indexes and partial atomic charges calculated with the electronic densities at the BLYP/DNP and BOP/DNP levels of theory. In the first system considered, that is, the $C_{59}HN$ molecule, according to the calculated $\Xi_{\Delta N \leq 0, \alpha}^K$ values, carbons 6 and its equivalent carbon 12 are the preferred sites for reacting with electrophiles. Then, carbon 18 is the most reactive site whose hydrogenation leads to 6,18-isomer of $C_{59}H_3N$. Finally, the predicted regioselectivity in $C_{59}H_4N$ and $C_{59}H_5N$ structures shows that 1,4-adducts are preferred for the addition of pairs of hydrogen atoms onto $C_{59}H_{n+1}N$ ($n = 0-4$) systems. We show that the multiple additions are only feasible up to a $C_{59}H_5N$ (tetraaddition) product; consequently, the application of this indicator helps to avoid systematic computational studies by comparing energies of formation in multiple isomers. A comparison with Fukui functions as well as with HOMO electron density suggests a better performance of the $\Xi_{\Delta N \leq 0, \alpha}^K$ indicator for predicting reactivity in molecules with multiple reactive sites, such as azafullerene derivatives.

Acknowledgment. F.F.C.-T. is grateful to the National Autonomous University of Mexico, UNAM, for a postdoctoral fellowship. Financial support from the National Autonomous University of Mexico (Grants DGAPA-IN101906 and -IN100107)

and from the National Council of Science and Technology of Mexico (Grants CONACYT-U48863-R and -56420) is greatly appreciated. We also thank Antonio Ramirez and Enrique Palacios from Computer Unit Staff of Instituto de Ciencias Nucleares for technical support.

References and Notes

- (1) Hummelen, J. C.; Bellavia-Lund, C.; Wudl, F. *Top. Curr. Chem.* **1999**, *199*, 93.
- (2) Hirsch, A.; Nuber, B. *Acc. Chem. Res.* **1999**, *32*, 795.
- (3) Hirsch, A.; Brettreich, M. *Heterofullerenes. Fullerenes, Chemistry and Reactions*, 2nd ed.; Wiley-VCH: Weinheim, Germany, 2005; Chapter 12, p 359.
- (4) Vostrowsky, O.; Hirsch, A. *Chem. Rev.* **2006**, *106*, 5191.
- (5) Reuther, U.; Hirsch, A. *Carbon* **2000**, *38*, 1539.
- (6) Tagmatarchis, N.; Shinohara, H. *Org. Lett.* **2000**, *2*, 3551.
- (7) Pichler, T.; Knupfer, M.; Golden, M. S.; Haffner, S.; Friedlein, R.; Fink, J.; Andreoni, W.; Curioni, A.; Keshavarz-K., M.; Bellavia, C.; Sastre, A.; Hummelen, J. C.; Wudl, F. *Phys. Rev. Lett.* **1997**, *78*, 4249.
- (8) Andreoni, W.; Gygi, F.; Parrinello, M. *Chem. Phys. Lett.* **1992**, *190*, 159.
- (9) Averdung, J.; Luftmann, H.; Schlachter, I.; Mattay, J. *Tetrahedron* **1995**, *51*, 6977.
- (10) Hummelen, J. C.; Knight, B.; Pavlovich, J.; Gonzales, R.; Wudl, F. *Science* **1995**, *269*, 1554.
- (11) Andreoni, W.; Curioni, A.; Holczner, K.; Prassides, K.; Keshavarz-K., M.; Hummelen, J.-C.; Wudl, F. *J. Am. Chem. Soc.* **1996**, *118*, 11335.
- (12) Parr, R. G.; Yang, W. *J. Am. Chem. Soc.* **1984**, *106*, 4049.
- (13) Yang, W.; Parr, R. G. *J. Chem. Phys.* **1984**, *81*, 2862.
- (14) Fukui, K. *Theory of Orientation and Stereoselection*; Springer-Verlag: New York, 1975.
- (15) Kohn, W.; Sham, L. J. *Phys. Rev. A* **1965**, *140*, 1133.
- (16) Parr, R. G.; Yang, W. *Density-Functional Theory of Atoms and Molecules*; Oxford UP: New York, 1989.
- (17) Ayers, P. W.; Levy, M. *Theor. Chem. Acc.* **2000**, *103*, 353.
- (18) Ayers, P. W.; Anderson, J. S. M.; Bartolotti, L. J. *Int. J. Quantum Chem.* **2005**, *101*, 520.
- (19) Geerlings, P.; De Proft, F.; Langenaeker, W. *Chem. Rev.* **2003**, *103*, 1793.
- (20) Chermette, H. *J. Comput. Chem.* **1999**, *20*, 129.
- (21) Parr, R. G.; Yang, W. T. *Annu. Rev. Phys. Chem.* **1995**, *46*, 701.
- (22) Bultinck, P.; Fias, S.; Alsenoy, C. V.; Ayers, P. W.; Carbó-Dorca, R. *J. Chem. Phys.* **2007**, *127*, 034102.
- (23) Yang, W.; Mortier, W. J. *J. Am. Chem. Soc.* **1986**, *108*, 5708.
- (24) Cohen, M. H.; Ganduglia-Pirovano, M. V.; Kudrnovský, J. *J. Chem. Phys.* **1994**, *101*, 8988.
- (25) Melin, J.; Ayers, P. W.; Ortiz, J. V. *J. Phys. Chem. A* **2007**, *111*, 10017.
- (26) Mendez, F.; Gazquez, J. L. *J. Am. Chem. Soc.* **1994**, *116*, 9298.
- (27) Gazquez, J. L.; Mendez, F. *J. Phys. Chem.* **1994**, *98*, 4591.
- (28) Li, Y.; Evans, J. N. S. *J. Am. Chem. Soc.* **1995**, *117*, 7756.
- (29) Anderson, J. S. M.; Melin, J.; Ayers, P. W. *J. Chem. Theory Comput.* **2007**, *3*, 358.
- (30) Anderson, J. S. M.; Melin, J.; Ayers, P. W. *J. Chem. Theory Comput.* **2007**, *3*, 375.
- (31) Liang, Y.; Wang, G.; Xu, X.; Cai, Z.; Pan, Y.; Zhao, X. *Phys. Chem. Chem. Phys.* **2003**, *5*, 1739.
- (32) Liang, Y.; Wang, G.; Xu, X.; Zhang, C.; Cai, Z.; Pan, Y.; Zhao, X. *J. Mol. Struct. (THEOCHEM)* **2003**, *622*, 203.
- (33) Dixon, D. A.; Matsuzawa, N.; Fukunaga, T.; Tebbe, F. N. *J. Phys. Chem.* **1992**, *96*, 6109.
- (34) Matsuzawa, N.; Dixon, D. A.; Fukunaga, T. *J. Phys. Chem.* **1992**, *96*, 7594.
- (35) Clare, B. W.; Kepert, D. L. *J. Mol. Struct. (THEOCHEM)* **1993**, *281*, 45.
- (36) Becker, L.; Evans, T. P.; Bada, J. L. *J. Org. Chem.* **1993**, *58*, 7630.
- (37) Perdew, J. P.; Parr, R. G.; Levy, M.; Balduz, J. L., Jr. *Phys. Rev. Lett.* **1982**, *49*, 1691.
- (38) Zhang, Y.; Yang, W. *Theor. Chem. Acc.* **2000**, *103*, 346.
- (39) Yang, W. T.; Zhang, Y. K.; Ayers, P. W. *Phys. Rev. Lett.* **2000**, *84*, 5172.
- (40) Ayers, P. W. *J. Math. Chem.* **2008**, *43*, 285.
- (41) Becke, A. D. *Phys. Rev. A* **1988**, *38*, 3098.
- (42) Lee, C.; Yang, W.; Parr, R. G. *Phys. Rev. B* **1988**, *37*, 785.
- (43) Tsuneda, T.; Suzumura, T.; Hirao, K. *J. Chem. Phys.* **1999**, *110*, 10664.
- (44) Delley, B. *J. Chem. Phys.* **1990**, *92*, 508.
- (45) Delley, B. *J. Chem. Phys.* **2000**, *113*, 7756.
- (46) Contreras-Torres, F. F.; Jalbout, A. F.; Jiménez-Fabian, I.; Amelines, O. F.; and Basiuk, V. A. *J. Phys. Chem. C* **2008**, *112*, 2736.

- (47) Contreras-Torres, F. F. *Comput. Mater. Sci.* **2008**, DOI: 10.1016/j.commatsci. 2008.03.031.
- (48) Note that the representation of ΔN is similar in eqs 1 and 2 as well as in eqs 8 and 9. However, the values of ΔN are constant and equal to 1 for computing eqs 8 and 9; meanwhile, for computing eqs 1 and 2, these values can be chosen according to the system studied. In this paper, the $C_{59}H_{n+1}N$ ($n = 0-4$) systems are considered as nucleophiles, so it is $\Delta N \leq 0$ (e.g., $-1 \leq \Delta N \leq 0$).
- (49) Fitzgerald, G. Accelrys Inc. Personal communication.
- (50) Dewar, M. J. S.; Maitlis, P. M. *J. Chem. Soc.* **1957**, 2521.
- (51) Anderson, J. S. M.; Ayers, P. W. *Phys. Chem. Chem. Phys.* **2007**, *9*, 2371.
- (52) Mulliken, R. S. *J. Chem. Phys.* **1955**, *23*, 1833.
- (53) Reed, A. E.; Curtiss, L. A.; Weinhold, F. *Chem. Rev.* **1988**, *88*, 899.
- (54) Besler, B. H.; Merz, K. M.; Kollman, P. A. *J. Comput. Chem.* **1990**, *11*, 431.
- (55) Singh, U. C.; Kollman, P. A. *J. Comput. Chem.* **1984**, *5*, 129.
- (56) Breneman, C. M.; Wiberg, K. B. *J. Comput. Chem.* **1990**, *11*, 361.
- (57) Hirshfeld, F. L. *Theor. Chim. Acta* **1977**, *44*, 129.
- (58) Maslen, E. N.; Spackman, M. *Aust. J. Phys.* **1985**, *38*, 273.
- (59) De Proft, F.; Van Alsenoy, C.; Peeters, A.; Langenaeker, W.; Geerlings, P. *J. Comput. Chem.* **2002**, *23*, 1198.
- (60) Ayers, P. W. *J. Chem. Phys.* **2000**, *113*, 10886.
- (61) Bultinck, P.; Ayers, P. W.; Fias, S.; Tiels, K.; Van Alsenoy, C. *Chem. Phys. Lett.* **2007**, *444*, 205.
- (62) Bultinck, P.; Van Alsenoy, C.; Ayers, P. W.; Carbo-Dorca, R. *J. Chem. Phys.* **2007**, *126*, 144111.
- (63) Roy, R. K.; Pal, S.; Hirao, K. *J. Chem. Phys.* **1999**, *110*, 8236.
- (64) Roy, R. K.; Hirao, K.; Pal, S. *J. Chem. Phys.* **2000**, *113*, 1372.
- (65) Ayers, P. W.; Morrison, R. C.; Roy, R. K. *J. Chem. Phys.* **2002**, *116*, 8731.
- (66) Ayers, P. W.; Parr, R. G. *J. Am. Chem. Soc.* **2000**, *122*, 2010.
- (67) Ayers, P. W.; Parr, R. G. *J. Am. Chem. Soc.* **2001**, *123*, 2007.
- (68) Bartolotti, L. J.; Ayers, P. W. *J. Phys. Chem. A* **2005**, *109*, 1146.
- (69) Stowasser, R.; Hoffmann, R. *J. Am. Chem. Soc.* **1999**, *121*, 3414.
- (70) Vasil'ev, Y. V.; Abzalimov, R. R.; Tuktarov, R. F.; Nasibullaev, S. K.; Hirsh, A.; Taylor, R.; Drewello, T. *Chem. Phys. Lett.* **2002**, *354*, 361.
- (71) Reuther, U.; Hirsch, A. *Chem. Commun.* **1998**, 1401.
- (72) Hauke, F.; Atalick, S.; Guldi, D. M.; Hirsch, A. *Tetrahedron* **2006**, *62*, 1923.

JP8047967